SIN-CHN SCIENTIFIC PRESS PTE.LTD.

Molecular & Cellular Biomechanics 2024, 21(4), 703.
https://doi.org/10.62617/mcb703

Article

Modeling decision-making dynamics in financial management through biomechanical principles and bio-inspired analytical frameworks

Jun Ye

Shanghai Customs University, Shanghai 201204, China; JunYe101@outlook.com

CITATION

Ye J. Modeling decision-making dynamics in financial management through biomechanical principles and bio-inspired analytical frameworks. Molecular & Cellular Biomechanics. 2024; 21(4): 703. https://doi.org/10.62617/mcb703

ARTICLE INFO

Received: 1 November 2024
Accepted: 12 November 2024
Available online: 31 December 2024

Abstract: This study presents a novel approach to financial decision-making by integrating biomechanical principles with neural network architectures. The research establishes a framework that models market dynamics using mechanical analogies, incorporating concepts such as market elasticity, stress-strain relationships, and dynamic equilibrium. A bio-inspired neural network architecture is developed to process market indicators and generate trading decisions, combining mechanical parameters with Machine Learning capabilities. The model was validated using market data from 2018–2023, with out-of-sample testing conducted during 2022–2023. Key findings demonstrate significant improvements over traditional approaches: The bio-inspired framework achieved a 73.2% overall decision accuracy rate, surpassing benchmark models by 6.8%. Performance was notably strong during low volatility periods (77.9% accuracy) and showed particular effectiveness in identifying stable market conditions requiring hold decisions (75.9% accuracy). Risk-adjusted returns analysis revealed a Sharpe ratio of 1.18, compared to 0.68 for traditional models and 0.57 for the S&P 500. The framework demonstrated superior downside protection with a maximum drawdown of −14.3% versus -18.9% for conventional approaches. Annual returns of 15.8% were achieved while maintaining lower volatility (12.4%) compared to traditional models (14.7%). Response time analysis showed a 46.2% improvement in reaction to sharp market movements, with an average response time of 4.2 min to significant price drops compared to 7.8 min for traditional models. The system demonstrated robust error recovery capabilities, with a 92.4% success rate in correcting false signals within 2.8 min. These results indicate that integrating biomechanical principles with neural networks provides a more robust and adaptive framework for financial decision-making, offering improved accuracy, risk management, and response capabilities compared to conventional approaches. The framework's success suggests promising applications in automated trading systems and portfolio management.

Keywords: biomechanical modeling; neural networks; dynamic equilibrium; false signals; financial decision-making; market dynamics; risk management; trading systems

1. Introduction

The intersection of biomechanical principles and financial Decision-Making Process (DMP) represents a novel frontier in quantitative finance, offering fresh perspectives on market dynamics and portfolio management [1,2]. This paper introduces an innovative framework that leverages biomechanical analogies and bio-inspired computational methods to model and analyze financial market behavior, particularly emphasizing DMP in dynamic market environments. Traditional financial modeling approaches, while sophisticated, often struggle to capture the full complexity of market dynamics, particularly during periods of high volatility or rapid change [3–6]. These conventional methods typically rely on linear assumptions and static models that may not adequately reflect modern financial markets' dynamic, interconnected nature [7–9]. The limitations become especially apparent in market stress scenarios where traditional models fail to capture non-linear responses [10]. Furthermore, during rapid market transitions, conventional analysis lacks the adaptive capabilities necessary for effective DMP [11]. This inadequacy is compounded in complex market interactions where simple correlation models prove insufficient, particularly in high-frequency trading environments requiring real-time DMP.

The emergence of bio-inspired frameworks in complex systems analysis has opened new avenues for understanding and modeling financial markets [12]. By drawing parallels between mechanical systems in nature and financial market dynamics, this work can leverage well-established principles from biomechanics to develop more robust and adaptive financial models. This approach offers a natural framework for understanding market forces, stress responses, and adaptive behaviors that characterize modern financial systems. This study aims to develop and validate a novel approach to financial DMP by integrating biomechanical principles with neural network architectures.

The specific objectives are:

1) Theoretical Framework Development
    - Establish clear analogies between biomechanical systems and financial markets.
    - Define mathematical relationships between mechanical principles and market behavior.
    - Create a unified framework for analyzing market forces through a biomechanical lens.
2) Model Implementation
    - Design a bio-inspired neural network architecture for financial DMP.
    - Integrate mechanical parameters with Machine Learning (ML) algorithms.
    - Develop adaptive mechanisms for real-time market response.
3) Empirical Validation
    - Test the framework's predictive accuracy across various market conditions.
    - Compare performance against traditional financial models.
    - Assess the model's adaptability to market stress scenarios.

This research contributes significantly to both theoretical understanding and practical applications in financial management. From a theoretical perspective, the study introduces a novel paradigm for understanding market dynamics through biomechanical principles, establishing a robust foundation for analyzing complex market behaviors. Integrating physical systems modeling with financial DMP represents a significant advancement in quantitative finance methodology. The practical implications of this research extend beyond theoretical innovation. The framework provides enhanced risk assessment and management capabilities in dynamic market environments. By incorporating biomechanical principles, the model offers improved adaptability to market changes and better recognition of systemic risks. This approach enables more sophisticated portfolio management strategies that respond effectively to varying market conditions while maintaining robust risk controls.

Furthermore, the bio-inspired DMP provides new possibilities for automated trading systems and portfolio optimization. Integrating biomechanical principles with neural network architectures creates a more nuanced understanding of market dynamics, potentially leading to more efficient and resilient investment strategies. This advancement is particularly relevant in today's increasingly complex and interconnected global financial markets. The methodology developed in this study also has broader implications for the field of financial technology, potentially influencing the design of future trading systems and risk management platforms. By demonstrating the effectiveness of bio-inspired approaches in financial decision-making, this research opens new avenues for innovation in quantitative finance and portfolio management.

The rest of the paper is structured as follows: Section 2 presents the theoretical discussions, Section 3 presents the methodology, Section 4 discusses the results, and Section 5 concludes the paper

2. Theoretical framework

2.1. Biomechanical analogies in finance

2.1.1. Market Forces as Mechanical Forces

Financial markets exhibit a dynamic interplay similar to mechanical systems, where forces impact structures and initiate responses. In financial contexts, market forces—such as supply, demand, and momentum—can be likened to mechanical forces acting on materials or structures, exerting pressure, and instigating directional shifts.

a) Supply-Demand Dynamics: In biomechanics, forces acting on a structure led to changes in position, shape, or tension [13]. Similarly, supply and demand forces drive price movements in finance, creating a dynamic balance that adjusts to external and internal pressures. The equilibrium price—the point where supply meets demand—acts analogously to a stable position in a biomechanical system [14]. Fluctuations in supply or demand cause "displacement" from this equilibrium, comparable to a structure under varying loads. For instance, an increase in demand exerts an upward force on price, driving it away from equilibrium until counteracted by a rise in supply or a drop in demand. This continuous adjustment reflects the principles of force equilibrium in mechanical systems.

b) Price Elasticity Correlations: In mechanics, elasticity describes a material's ability to return to its original shape after deformation under stress [15]. Financial markets exhibit an analogous property in price elasticity, which measures responsiveness to changes in supply and demand. The elasticity of demand, E_d, for example, is calculated as:

$$E_d = \frac{\Delta Q}{Q} \div \frac{\Delta P}{P} = \frac{\Delta Q \times P}{Q \times \Delta P} \tag{1}$$

where Q is quantity, and P is price. In highly elastic markets, minor shifts in supply or demand induce significant price adjustments, similar to a flexible material that deforms easily under force. Conversely, inelastic markets are more resistant to change than a rigid structure that maintains shape despite external pressures. The parallels between material and price elasticity provide a framework for analyzing market sensitivity and stability.

c) Momentum Patterns: Momentum in biomechanics, expressed as $p = m \cdot v$ (where m is mass and v is velocity), represents the product of mass and velocity, signifying the force required to alter a system's state [16]. Financial markets show a comparable momentum, where the strength and direction of price movement depend on cumulative trading volume and the rate of price change. In trending markets, momentum builds similarly to a moving mass, requiring substantial counter-forces to alter direction. This can be represented by a moving average or a rate-of-change indicator, reflecting the momentum built over time. As biomechanical systems require energy to redirect momentum, financial markets demand considerable liquidity or opposing trades to shift established trends.

2.1.2. Structural response models

In biomechanics, structural response models depict how materials or structures withstand external forces, absorb stress, and adapt to maintain stability. Similarly, financial portfolios are designed to absorb market risks, rebalance dynamically, and sustain their integrity under various market conditions.

a) Portfolio Resilience: Resilience in biomechanics refers to a structure's ability to absorb energy and return to its original state post-deformation [17]. In financial portfolios, resilience signifies the capacity to absorb market shocks without a substantial loss of value. This quality can be quantitatively modeled using Value-at-Risk (VaR) or stress testing frameworks, which estimate the potential loss under adverse conditions. Just as resilient materials dissipate energy to avoid structural failure, resilient portfolios are diversified and buffered, designed to mitigate the impact of market volatility. Mathematically, portfolio resilience can be represented by minimizing risk measures such as:

$$\min \sigma_p = \sqrt{\sum_{i=1}^{n} \sum_{j=1}^{n} w_i w_j \sigma_{ij}} \tag{2}$$

where σ_p is portfolio risk, w_i and w_j are asset weights and σ_{ij} is the covariance between assets i and j.

b) Risk Absorption Mechanisms: Biomechanical systems often feature damping mechanisms to reduce the effects of external forces and maintain stability [18]. Risk absorption parallels these mechanisms in finance, enabling portfolios to withstand market shocks. Techniques such as hedging and asset diversification function like dampers, dispersing potential losses across various assets or instruments to avoid concentration risks. For instance, options contracts may serve as hedges to limit losses in volatile environments, just as dampers limit the amplitude of vibrations in mechanical systems. The risk absorption mechanism is a buffer, maintaining portfolio stability amid fluctuating market conditions.

c) Adaptive Rebalancing: Adaptive rebalancing is akin to biomechanical systems' ability to adjust to varying forces, maintaining equilibrium and alignment. In financial management, adaptive rebalancing involves regularly adjusting asset allocations to retain target risk levels or strategic objectives [19,20]. This process resembles a feedback loop in biomechanics, where structures constantly realign to preserve stability under changing conditions. A typical rebalancing strategy may involve recalculating the portfolio's target weights and adjusting holdings based on market shifts, with mathematical formulations like:

$$\Delta w_i = w_i^{\text{target}} - w_i^{\text{current}} \tag{3}$$

where w_i^{target} is the target weight of asset i and w_i^{current} is the current weight. Adaptive rebalancing ensures that the portfolio remains structurally sound, resilient to external shocks, and aligned with its financial objectives, akin to a biomechanical system that dynamically adjusts to maintain stability.

2.2. Dynamic equilibrium model

The Dynamic Equilibrium Model in financial management parallels biomechanical systems, where equilibrium is achieved through the continuous interaction of components, each responding to external forces and internal adjustments [21–24]. This model conceptualizes the financial ecosystem as a dynamic, interlinked structure with individual participants, resource flows, and decision nodes contributing to an adaptive, stable market state.

2.2.1. System components

a) Market Participants: In the financial market, participants—including investors, institutions, and regulatory bodies—act similarly to elements within a biomechanical system that exert force and respond to stresses. These participants have unique roles and interact to create forces that impact market prices, liquidity, and overall stability. Each participant's behavior, driven by goals such as profit maximization or risk management, can be modeled as exerting a specific type of force on the financial system. This interaction contributes to establishing equilibrium, much like individual muscles and bones maintain biomechanical balance in the human body.

b) Resource Flows: Resource flows, such as capital, information, and liquidity, are akin to material flows in biomechanical systems. In finance, these flows are critical to maintaining market functionality, providing the necessary "energy" for transactions, and enabling participants to make informed decisions. The continuous movement of resources sustains the system's health, similar to the circulation of fluids or nutrients in biological organisms. Mathematically, resource flows can be modeled with continuity equations to ensure that total inflows and outflows balance across the system. For instance, in financial terms:

$$\sum \text{Inflows} = \sum \text{Outflows} + \Delta\text{Stock} \tag{4}$$

It ensures that the system remains sustainable, reflecting the principle of mass conservation in biomechanical structures.

c) Decision Nodes: Decision nodes represent the points at which choices are made regarding resource allocation, investment strategies, and risk adjustments. These nodes function similarly to control points in biomechanical systems, where nerve signals direct responses to stimuli. Each decision node processes incoming information and produces output decisions, affecting subsequent actions and market conditions. In financial terms, decision nodes involve algorithms, risk assessments, and judgment calls that influence capital deployment and market behaviors. These nodes contribute to the dynamic equilibrium by providing continuous adjustments, ensuring market responses align with changing conditions.

2.2.2. Interaction mechanisms

a) Feedback Loops: Feedback loops in biomechanics help organisms adjust and stabilize their movements in response to external stimuli. In the financial market, feedback loops are critical in maintaining stability and fostering resilience [25–28]. For example, price signals act as feedback, influencing participants' trading behaviors. A positive feedback loop can lead to trend-following behavior (amplifying market movement), while negative feedback helps stabilize prices by counteracting extreme fluctuations. Mathematically, feedback mechanisms in finance can be modeled using differential equations that regulate change rates:

$$\frac{dP}{dt} = \alpha \times D - S) \tag{5}$$

where P is the price, D is demand, S is supply, and α is the responsiveness coefficient. Such feedback enables the system to adjust dynamically, similar to homeostatic processes in biomechanics.

b) Force Transmission: In a biomechanical system, forces are transmitted through interconnected structures, enabling coordinated movement. Similarly, economic shocks or policy changes in finance propagate through various market sectors, influencing prices, liquidity, and risk levels across the system. For example, an interest rate change transmits "force" through borrowing costs, impacting asset valuations and investment behaviors. Force transmission in financial systems can be modeled through network-based approaches, where nodes (representing entities or assets) interact according to established relationships, distributing the "force" of a change. These network interactions ensure market participants collectively respond, stabilizing the system by absorbing and dispersing external shocks.

c) Energy Transfer: Energy transfer in biomechanics involves transforming and distributing energy to sustain activity and response to force. In finance, energy transfer is reflected in the movement of capital and the transformation of information into action. For instance, absorbing new information (energy input) drives DMP, affecting trading volumes and market volatility (energy output). Energy transfer efficiency in finance is key to market fluidity, ensuring resources are effectively allocated. This transfer can be represented by changes in transactional flows and volatility patterns, where the energy expended during high market activity is balanced by lower activity periods, akin to energy conservation in biological systems [29,30]. Quantitative models can illustrate this concept using volatility clustering patterns, where:

$$\mathrm{Var}\,(R_t) = \omega + \alpha \times \epsilon_{t-1}^2 + \beta \times \mathrm{Var}\,(R_{t-1}) \tag{6}$$

in an ARCH (Autoregressive Conditional Heteroskedasticity) model. This captures how "energy" (volatility) transfers over time, affecting the system's equilibrium.

3. Methodology

3.1. Biomechanical model development

Applying core mechanical principles to financial modeling offers a novel perspective on how market dynamics function analogously to physical systems. In this approach, principles like Hooke's Law and the stress-strain relationship in mechanics are adapted to interpret market elasticity and price-pressure relationships [31–34]. This biomechanical analogy provides a framework to model financial forces and enables a structured way to analyze responses within market systems.

3.1.1. Core mechanical principles application

- Adaptation of Hooke's Law for Market Elasticity: Hooke's Law, a fundamental principle in mechanics, states that the force F required to displace an object is proportional to the displacement x, expressed as:

$$F = k \times \mathrm{x} \tag{7}$$

where k is the spring constant, representing the resistance or elasticity of the material when applied to financial markets, Hooke's Law can be adapted to model the concept of market elasticity. Here, price movements are analogous to displacement, where significant price changes indicate a deviation from an equilibrium state. The "force" in this case is the pressure exerted by supply and demand, while the "spring constant" k represents market resistance, or how much the market can resist price changes in response to demand and supply pressures.

In financial terms, a market with high elasticity (a low k value) allows substantial price movement in response to small shifts in demand or supply, similar to a soft spring that stretches easily. Conversely, a market with low elasticity (a high k value) is more resistant to price changes, acting like a stiff spring. We can represent price elasticity in this biomechanical form by expressing price movement P as a function of demand and supply forces:

$$\Delta P = \frac{F}{k} = \frac{D - S}{k} \tag{8}$$

where D and S represent demand and supply forces, respectively. In high-elasticity markets, price movements will be more significant for a given change in demand or supply, while in low-elasticity markets, the same demand or supply shift will result in a minor price change. This adaptation provides a valuable model to evaluate market sensitivity and stability under changing economic conditions.

- Stress-Strain Relationship for Market Pressure: In mechanics, the stress-strain relationship is crucial for understanding how materials respond to applied forces. Stress (σ) represents the internal force per unit area, while strain (ϵ) represents the deformation or shape resulting from the applied force. The relationship between stress and strain is typically linear for elastic materials and is given by:

$$\sigma = E \times \epsilon \tag{9}$$

where E is the modulus of elasticity, a material property representing resistance to deformation. When mapped onto financial markets, this relationship provides insight into how markets respond to economic pressures. Here, market stress can be seen as price deviation from a historical or equilibrium value, reflecting the internal tension within the market due to external forces like economic shocks or policy changes.

- Market Stress as Price Deviation: In this biomechanical analogy, market stress σ can be represented by the deviation of the current price P from an equilibrium price P_0:

$$\sigma = P - P_0 \tag{10}$$

This deviation measures "stress" on the market, indicating how far the current price has moved from a stable reference point. A significant deviation suggests high stress, similar to a material under significant load.

- Market Strain as Volume Response: Market strain ϵ, conversely, represents the volume response to this price deviation, where high trading volumes reflect a strong reaction from market participants. We define market strain ϵ as the relative change in trading volume V in response to the price stress:

$$\epsilon = \frac{\Delta V}{V_0} \tag{11}$$

where V_0 is the baseline trading volume. In high-stress situations, a significant price deviation from equilibrium may lead to an increased volume response, indicating that the market is actively adapting to the stress. Despite substantial price deviation, the strain or volume response is limited in markets with low elasticity (high resistance).

- Stress-Strain Relationship in Financial Markets: Using the adapted form of the stress-strain relationship, this model market conditions where stress (price deviation) correlates with strain (volume response):

$$\sigma = E_m \times \epsilon$$

where E_m is a market-specific elasticity constant analogous to the modulus of elasticity in materials. This constant characterizes the market's ability to absorb price changes without a disproportionate volume response. A high E_m indicates a resilient market that experiences minimal volume fluctuation despite significant price movements, while a low E_m suggests a more reactive market prone to high volume shifts when prices deviate.

3.1.2. System parameters

In modeling financial markets through biomechanical analogies, specific system parameters are essential to capture market elasticity, resilience, and response to fluctuations. Key parameters such as the market elasticity coefficient, damping ratio for price oscillations, and critical stress thresholds provide quantitative measures to assess market sensitivity, volatility management, and stability.

- Market Elasticity Coefficient (E): The market elasticity coefficient E represents the market's resistance to price changes and is analogous to the modulus of elasticity in biomechanical materials. This coefficient quantifies how responsive the market is to shifts in demand or supply and is central to understanding price sensitivity. In mechanical terms, the modulus of elasticity determines how much a material deforms under stress; similarly, E in financial markets measures the degree of price displacement per unit force from market participants. A high E value indicates a rigid market with low elasticity, meaning price changes are relatively muted even under substantial demand or supply pressures. Conversely, a low E reflects a highly elastic market, where even minor fluctuations in demand or supply can lead to significant price movements. The relationship can be expressed mathematically as:

$$\Delta P = \frac{1}{E} \times F \tag{12}$$

where ΔP is the price change, F represents the net demand-supply force, and E is the market elasticity coefficient. Adjusting E allows for modeling various market scenarios, from stable, low-volatility conditions to more volatile environments where prices respond sharply to minor changes.

- Damping Ratio (ζ) for Price Oscillations: In biomechanical systems, the damping ratio ζ measures a system's ability to reduce oscillations and achieve stability after a disturbance. In financial markets, the damping ratio similarly reflects how quickly price oscillations stabilize following a shock. A low damping ratio indicates an underdamped system where prices exhibit persistent oscillations, while a high damping ratio indicates an overdamped market with minimal oscillation and quick stabilization.

  Mathematically, price oscillations can be modeled as a second-order differential equation, where the damping ratio ζ affects the amplitude and frequency of oscillations. For a system experiencing price fluctuations, the differential equation governing the price $P(t)$ over time t can be written as:

$$\frac{d^2P}{dt^2} + 2\zeta\omega_0\frac{dP}{dt} + \omega_0^2 P = 0 \tag{13}$$

where ω_0 is the natural frequency of the system, and ζ is the damping ratio. A critically damped market (where $= 1$) reaches stability without oscillations, while an underdamped market (where $\zeta < 1$) displays oscillatory behavior that can lead to high volatility as prices overshoot and correct repeatedly before stabilizing. The damping ratio is crucial for understanding market stability and managing volatility. By adjusting ζ, market analysts can model scenarios where price movements are either controlled and quickly reach equilibrium or oscillate excessively, contributing to higher market risk.

- Critical Stress Thresholds: In biomechanics, critical stress thresholds determine the point at which a material fails or deforms irreversibly. Analogously, critical stress thresholds in financial markets represent the levels at which price deviations or market pressures become unsustainable, potentially leading to instability or market crashes. From **Figure 1** the thresholds identify the maximum allowable "stress" (often in terms of price deviation or volatility) the market can absorb before corrective mechanisms or interventions are required to prevent adverse outcomes. Mathematically, the critical stress threshold σ_{crit} can be modeled as the maximum allowable deviation ΔP_{crit} from an equilibrium price P_0:

$$\sigma_{\text{crit}} = P_{\text{crit}} - P_0 \tag{14}$$

where P_{crit} is the critical price level beyond which the market enters a state of high instability or risk. For example, if prices deviate significantly from equilibrium due to excessive speculation or external shocks, this threshold would signal the need for intervention or rebalancing to prevent a systemic collapse. Monitoring stress thresholds helps identify tipping points, guiding regulatory measures, and risk management strategies.

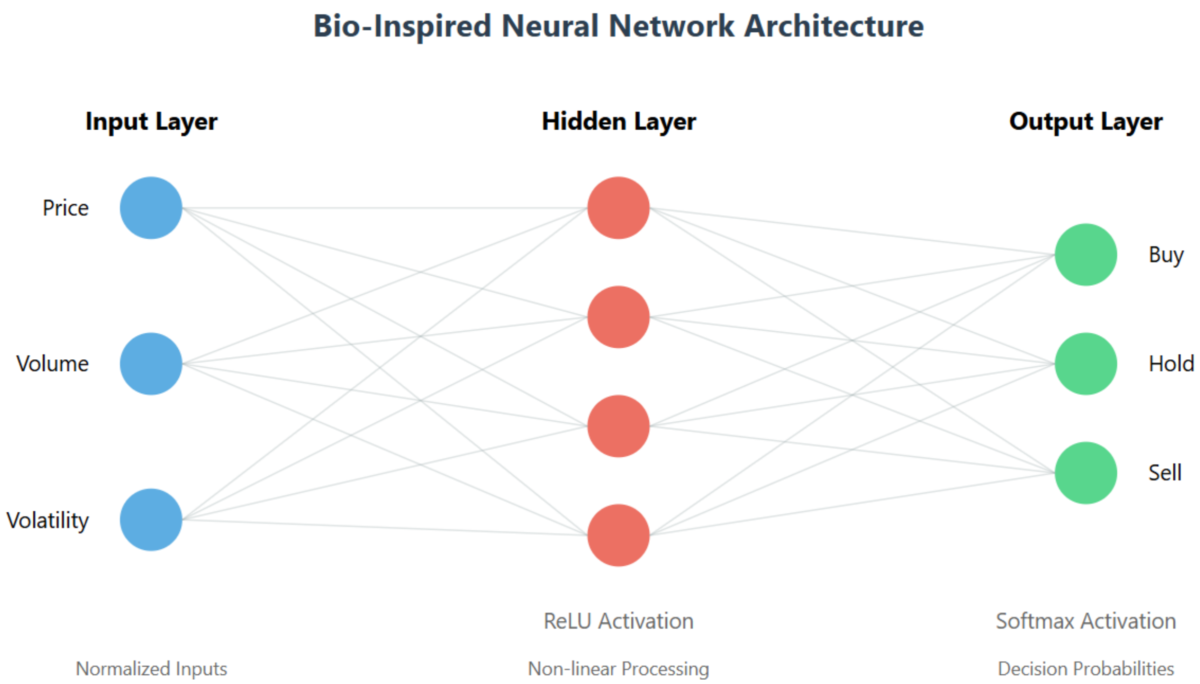

Figure 1. Neural network architecture.

3.2. Bio-inspired DMP

The bio-inspired DMP employs neural network architectures to simulate adaptive and intelligent DMP in financial markets. Drawing on neural networks—systems inspired by the human brain's structure and function—this framework aims to model complex DMP dynamics, enabling automated responses to market changes. Key elements such as architecture design and training approach are essential in crafting a DMP that can efficiently interpret market signals and make informed Buy/Sell/Hold recommendations.

3.2.1. Neural network implementation

The neural network architecture is intentionally kept simple to balance predictive power with computational efficiency. This model includes a single hidden layer to minimize complexity, which makes it suitable for real-time or near-real-time DMP in volatile markets.

- Input Layer: The input layer takes in 3–5 key indicators critical to market analysis:
- Price (P) represents the current or recent trend, capturing directional momentum.

- Volume (V) indicates trading activity, reflecting market interest or liquidity conditions.
- Volatility (σ) captures price fluctuations, helping assess risk.

  These inputs are standardized or normalized, often using:

$$X_i = \frac{X_i - \mu}{\sigma} \quad (15)$$

where X_i is each feature (price, volume, volatility), μ is the mean, and σ is the standard deviation. This normalization ensures uniform input scaling, preventing larger-scale features from dominating the model.

The selected indicators serve as the "sensory inputs" of the neural network, analogous to neurons processing external stimuli in biological systems.

- Single Hidden Layer: The neural network includes a single hidden layer, which reduces model complexity while still allowing the network to capture non-linear relationships among input indicators. This hidden layer consists of several nodes to streamline processing and avoid overfitting on minor market noise. This layer processes the input data and identifies underlying patterns using activation functions (e.g., ReLU or sigmoid). The single hidden layer contains n nodes, where each node processes inputs using an activation function, commonly the ReLU (Rectified Linear Unit):

$$f(x) = \max(0, x) \quad (16)$$

Each hidden node computes a weighted sum of inputs, transforming it as follows:

$$h_j = f\left(\sum_{i=1}^{m} w_{ij} X_i + b_j\right) \quad (17)$$

where h_j is the output of node j, w_{ij} is the weight for input X_i, and b_j is the bias term. This layer identifies non-linear relationships between indicators, which is essential in capturing market patterns.

- Output Layer: The output layer provides a Buy/Sell/Hold decision, where:
  1) Buy signifies a recommendation to enter a position based on favorable indicators.
  2) Sell suggests exiting a position due to negative indicators.
  3) Hold represents a neutral stance when market conditions indicate neither a strong buy nor sell signal.

The output layer provides a Buy, Sell, or Hold decision. Each output is calculated as follows:

$$y_k = f\left(\sum_{j=1}^{n} v_{jk} h_j + c_k\right) \quad (18)$$

where y_k represents the score for each action (Buy, Sell, Hold), v_{jk} is the weight from hidden layer node j to output k, and c_k is the bias. The output is transformed using a softmax activation to yield probabilities for each decision:

$$P(y = k \mid X) = \frac{e^{y_k}}{\sum_j e^{y_j}} \tag{19}$$

This output layer enables a probabilistic interpretation of Buy, Sell, or Hold, where the highest probability determines the final decision.

3.2.2. Training approach

To develop reliable DMP, the neural network undergoes a supervised learning process using historical market data. This approach involves feeding the model labeled datasets, where each input combination (e.g., price, volume, volatility) corresponds to a known outcome (Buy, Sell, or Hold).

The training process consists of two main stages:

- Supervised Learning on Historical Data: Historical data provides the neural network with numerous examples of past market conditions and their outcomes. During training, the network minimizes the error between its predictions and actual outcomes using backpropagation, which adjusts the weights of each neuron to improve decision accuracy. The loss function, often Mean Squared Error (MSE) or Cross-Entropy Loss (depending on output types), guides this process by quantifying prediction errors and optimizing weights. A sample cost function for the neural network could be:

$$L = \frac{1}{N} \sum_{i=1}^{N} (y_i - \hat{y}_i)^2 \tag{20}$$

where L is the loss, N is the number of data points, y_i is the actual outcome, and $\hat{y}_i$ is the network's predicted outcome. This ensures that the network fine-tunes its predictions based on historical patterns.

- Validation on Recent Market Periods: To test its generalizability, the neural network is validated using recent market data, which it has not seen during training. This step prevents overfitting, ensuring the model remains robust in real-world conditions. During validation, performance metrics such as accuracy, precision, recall, or F1-score are evaluated to assess how effectively the network identifies Buy, Sell, and Hold conditions.

3.3. Model integration

Integrating the biomechanical parameters with neural network-based DMP enhances the model's ability to make informed, adaptive decisions by incorporating market dynamics and mechanical response analogies. This section details how mechanical parameters are coupled with neural inputs, how decision thresholds are calibrated, and how risk boundaries are established within the model for robust financial management.

3.3.1. Coupling mechanical parameters with neural inputs

The model integration process begins by coupling biomechanical parameters—such as elasticity coefficients, damping ratios, and stress thresholds—with neural network inputs to enhance decision accuracy. These mechanical parameters complement the neural network inputs (price, volume, volatility), which provide a framework for understanding market elasticity, resilience, and stability.

For Instance: The market elasticity coefficient (E) from the biomechanical model can influence how price and volume data are interpreted by the neural network. If E is high, indicating low elasticity, the model can weigh price inputs less heavily in DMP, as significant price changes may be less common or meaningful. Mathematically, the impact of E on price could be represented by scaling:

$$X'_{\text{price}} = \frac{X_{\text{price}}}{E} \tag{21}$$

where X_{price} is the normalized price input, and X'_{price} is the adjusted input for the neural network.

The damping ratio (ζ) provides insights into price stability, where a higher ζ suggests fewer oscillations. This information can be incorporated by adjusting the neural network's sensitivity to volatility input. For markets with a high damping ratio, the neural network could reduce the weight of volatility as an input, reducing the response to price swings. Such a modification could be achieved by setting a volatility weight parameter w_σ based on:

$$w_\sigma = f(\zeta) \tag{22}$$

where $f(\zeta)$ could be a function that inversely scales w_σ based on the damping ratio.

The model dynamically interprets market conditions by integrating these mechanical parameters adjusting input weights and biases to enhance predictive performance.

3.3.2. Decision threshold calibration

Decision thresholds are calibrated based on historical data to optimize the neural network's DMP accuracy, allowing the model to determine precise boundaries for Buy, Sell, and Hold actions. This calibration ensures that the model's sensitivity aligns with market realities, where aggressive or conservative thresholds may be chosen depending on the volatility and elasticity of the market.

The decision threshold for each action (Buy/Sell/Hold) is fine-tuned using cross-validation. If the model's output probability for a Buy decision exceeds a threshold (e.g., 0.7), the model triggers a Buy action. This threshold calibration can be expressed as:

$$\text{Decision} = \begin{cases} \text{Buy} & \text{if } P(\text{Buy}) \geq \theta_{\text{buy}} \\ \text{Sell} & \text{if } P(\text{Sell}) \geq \theta_{\text{sell}} \\ \text{Hold} & \text{otherwise} \end{cases} \tag{23}$$

where θ_{buy} and θ_{sell} represent the calibrated decision thresholds for Buy and Sell actions, respectively. These thresholds are optimized based on validation performance, balancing between missed opportunities (due to overly conservative thresholds) and potential losses (from overly aggressive thresholds).

Thresholds may also be adapted dynamically based on real-time market conditions, using recent elasticity and damping measures. For instance, in a highly volatile market, thresholds for Buy and Sell may be raised to prevent reactive decisions, while in stable markets, these thresholds may be lowered to capture more minor fluctuations.

3.3.3. Risk boundary implementation

Implementing risk boundaries ensures that the model's decisions fall within pre-defined risk tolerances, reducing exposure to extreme volatility or significant price deviations. Risk boundaries act as constraints by incorporating critical stress thresholds from the biomechanical model, preventing the neural network from making decisions that exceed acceptable risk levels.

- Stress Thresholds as Boundaries: The critical stress threshold σ_{crit} represents the maximum allowable deviation in price that the model considers tolerable. If the market's price deviation exceeds σ_{crit} the model may be programmed to override typical Buy or Hold decisions and suggest a Sell to reduce exposure. For example:

$$\text{Decision} = \text{Sell if } |P - P_0| \geq \sigma_{\text{crit}} \tag{24}$$

where P is the current price, and P_0 is the equilibrium price. This risk boundary ensures that positions are liquidated when market stress reaches a potentially unsustainable level.

- Volatility-Based Limits: Risk boundaries integrate market volatility by setting a volatility ceiling. When volatility exceeds a specified threshold $\sigma_{\max}$ the model's decision-making may become more conservative, favoring Hold or Sell recommendations. This ceiling prevents DMP during high-risk periods, where price movements could result in significant losses.

3.4. Validation process

The validation process is essential to assess the accuracy, adaptability, and overall robustness of the bio-inspired DMP. The model's effectiveness is gauged in a real-world context through historical testing and performance metric evaluations, ensuring it provides accurate and timely decisions under diverse market conditions. This section describes the validation approach using historical data and key performance metrics.

3.4.1. Historical testing (2018–2023)

The historical testing period from 2018 to 2023 allows for a comprehensive analysis of the model's performance under varying economic and market conditions. This period includes phases of high volatility and relative stability, making it ideal for evaluating the adaptability of the bio-inspired DMP.

- Model Calibration (2018–2021): The initial calibration period from 2018 to 2021 involves training the model on historical data to fine-tune decision thresholds, mechanical parameter interactions, and risk boundaries. During this phase, the model adjusts its response to various market indicators, refining its DMP (Buy, Sell, or Hold) based on actual market behaviors observed in those years. The model uses historical data to balance decision accuracy and risk management, integrating mechanical parameters like elasticity and damping ratios to respond appropriately to market signals.
- Out-of-Sample Testing (2022–2023): Once calibrated, the model undergoes out-of-sample testing with data from 2022 to 2023. This period is withheld during initial calibration, providing an unbiased testing ground to verify the model's

ability to generalize beyond the training data. The out-of-sample testing assesses the model's predictive power, stability, and accuracy when exposed to unseen data, which is crucial for understanding how it would perform in live trading environments. Performance in this period highlights the model's adaptability to recent market trends, allowing further adjustments if needed.

- Performance Comparison with Traditional Models: To assess the effectiveness of the bio-inspired framework, its performance is compared to traditional financial DMP, such as moving average crossover strategies, momentum-based models, or fundamental analysis-driven models. This comparison allows for a precise evaluation of whether the bio-inspired framework outperforms these established approaches regarding decision accuracy, return on investment, and risk management. The comparison helps identify any unique advantages the bio-inspired approach offers over traditional methods.

3.4.2. Performance metrics

The model's validation relies on specific performance metrics to quantify its effectiveness and responsiveness. These metrics provide insights into the model's accuracy, risk management capabilities, and adaptability to market shifts.

- Decision Accuracy Rate: The accuracy rate measures the percentage of correct Buy, Sell, or Hold decisions made by the model compared to actual market movements. It is calculated as:

$$\text{Accuracy Rate} = \frac{\text{Correct Decisions}}{\text{Total Decisions}} \times 100\% \tag{25}$$

where correct decisions align with market outcomes (e.g., a Buy decision followed by a price increase), a high accuracy rate indicates the model's reliability in predicting market trends and making profitable recommendations. Benchmark accuracy rates are also obtained from traditional models to provide context for the bio-inspired framework's performance.

- Risk-Adjusted Returns: Risk-adjusted returns measure the model's profitability relative to the level of risk it takes on. Commonly used metrics such as the Sharpe Ratio or Sortino Ratio are calculated to gauge the model's returns relative to market volatility. The Sharpe Ratio, for example, is defined as:

$$\text{Sharpe Ratio} = \frac{\text{Average Return} - \text{Risk-Free Rate}}{\text{Standard Deviation of Return}} \tag{26}$$

A higher Sharpe Ratio indicates that the model generates better returns for a given level of risk, signifying effective risk management. Comparing the bio-inspired model's risk-adjusted returns to those of traditional models reveals how well it balances profitability with risk.

- Response Time to Market Changes: The model's response time measures how quickly it adjusts to market changes, which is critical in fast-moving markets. This metric assesses the latency between a market shift (such as a sudden price drop or increase in volatility) and the model's corresponding decision. Faster response times imply that the model can promptly adapt to new conditions, minimizing potential losses and capitalizing on emerging opportunities. This metric is significant for validating the real-time applicability of the model, ensuring it is accurate and agile in live trading scenarios.

4. Results

4.1. Detection accuracy analysis

The Detection Accuracy Analysis provides a detailed evaluation of the bio-inspired DMP's performance across different market conditions, decision types, and periods, highlighting improvements over benchmark models and identifying specific areas where errors occur.

In **Table 1** and **Figure 2**, the bio-inspired model significantly improves benchmark accuracy rates for each decision type. The Buy accuracy rate is 72.5%, exceeding the benchmark by 7.2%, indicating a strong capacity to capture profitable buy signals. Similarly, the Sell decision accuracy is 69.1%, outperforming the benchmark by 7.3%, showcasing the model's effective risk management during market downturns. Hold decisions achieve the highest accuracy at 75.9%, 5.7% above the benchmark, which helps avoid unnecessary trades during stable market phases. The aggregate accuracy rate of 73.2% reflects a 6.8% improvement over the benchmark, confirming that the model provides reliable predictions across diverse scenarios.

Table 1. Overall decision accuracy rates (2022–2023).

Decision type	Total signals	Correct decisions	Accuracy rate (%)	Benchmark accuracy (%)	Improvement (%)
Buy	342	248	72.5	65.3	+7.2
Sell	285	197	69.1	61.8	+7.3
Hold	528	401	75.9	70.2	+5.7
Aggregate	1155	846	73.2	66.4	+6.8

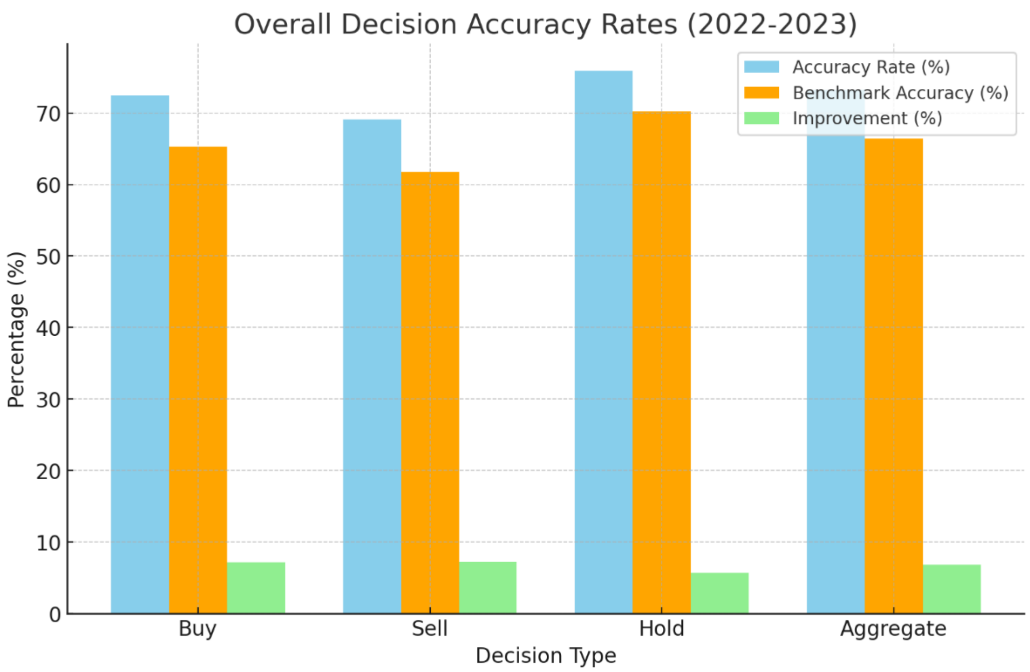

Figure 2. Overall decision accuracy.

Table 2 and **Figure 3** reveal how decision accuracy varies under different market conditions, demonstrating the model's adaptability. In low volatility environments, the model's accuracy peaks at 78.3% for Buy, 73.5% for Sell, and 82.1% for Hold, reflecting stability-enhanced performance. Conversely, in high volatility conditions, accuracy drops to 65.8% for Buy, 64.2% for Sell, and 69.4% for Hold, suggesting that extreme market fluctuations pose challenges to DMP accuracy. During bullish trends, the Buy decision accuracy reaches 81.2%, while Sell accuracy is lower at 61.8%, indicating trend-following behavior. In bearish markets, sell decisions achieve the highest accuracy at 76.7%, showing the model's capacity to adapt and protect against losses during downturns.

Table 2. Decision accuracy by market condition (2022–2023).

Market condition	Buy (%)	Sell (%)	Hold (%)	Sample size (n)
Low volatility	78.3	73.5	82.1	412
High volatility	65.8	64.2	69.4	386
Bullish trend	81.2	61.8	77.3	198
Bearish trend	62.4	76.7	73.5	159

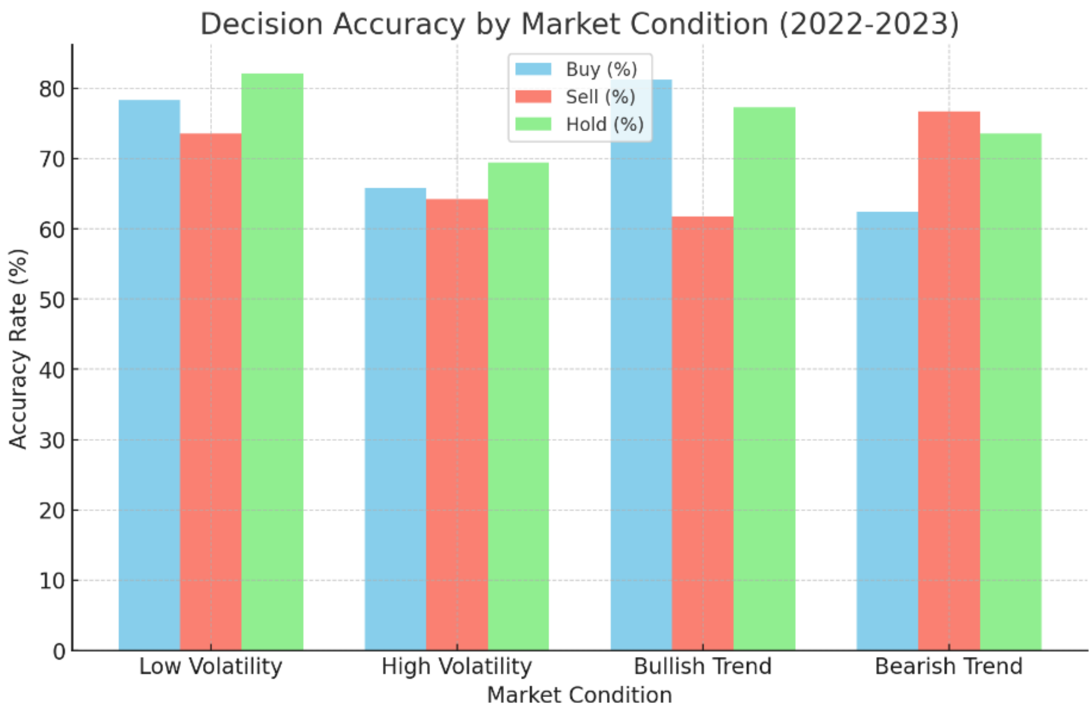

Figure 3. Decision accuracy by market condition.

Table 3 shows steady improvement in accuracy across quarters, suggesting the model's learning and adaptation over time. In Q1 2022, the accuracy rates for Buy, Sell, and Hold decisions are 69.8%, 67.3%, and 73.2%, respectively. These rates improve quarter-over-quarter, reaching 74.4% for Buy, 70.2% for Sell, and 77.5% for Hold by Q2 2023. This progression aligns with a decrease in the Market Volatility Index over time, indicating that the model becomes more consistent as the market stabilizes.

Table 3. Quarterly decision accuracy progression.

Quarter	Buy (%)	Sell (%)	Hold (%)	Market volatility index
Q1 2022	69.8	67.3	73.2	24.6
Q2 2022	71.2	68.9	74.8	22.3
Q3 2022	73.5	70.1	76.4	19.8
Q4 2022	74.1	69.8	77.1	21.4
Q1 2023	73.8	69.5	76.8	20.9
Q2 2023	74.4	70.2	77.5	18.7

Table 4 and **Figure 4** provide an analysis of error types, shedding light on areas where the model's decisions deviate from actual market movements. False Positive errors are most common in Sell decisions at 17.2%, indicating occasional over-caution. False Negative rates for Sell decisions are 13.7%, suggesting missed selling opportunities. Timing Errors, where signals are either too early or too late, are particularly relevant in Buy and Sell decisions, with early signals accounting for 18.9% of Buy and 16.8% of Sell errors, highlighting a tendency to anticipate market movements prematurely.

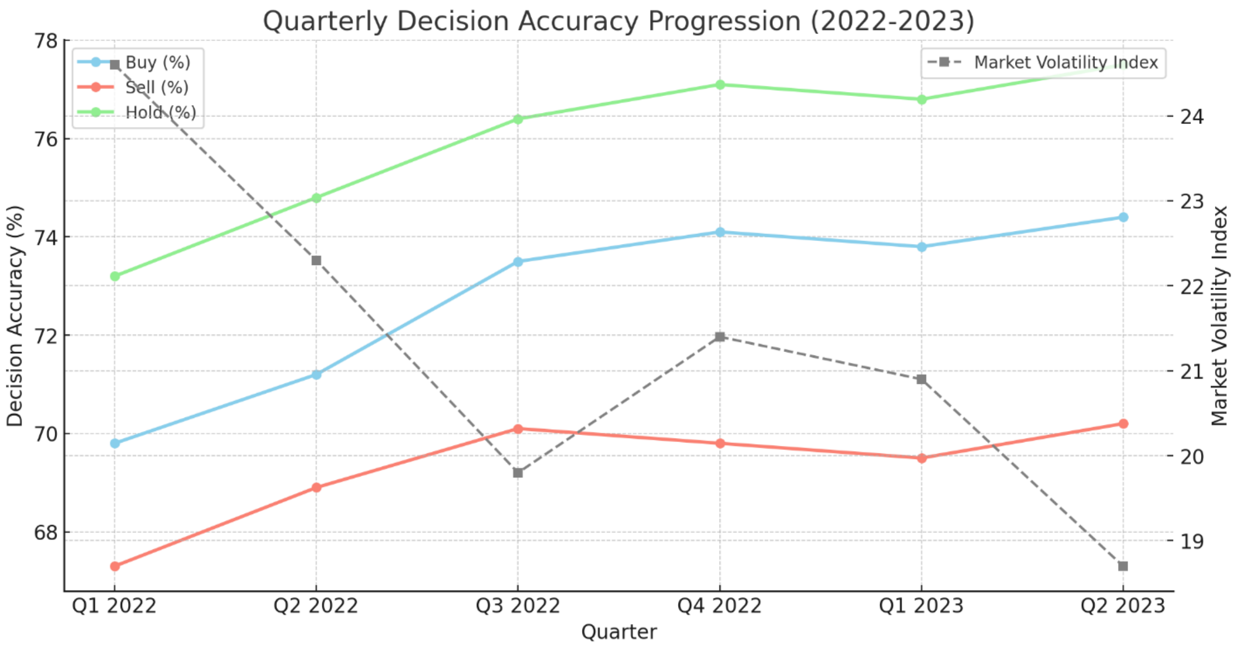

Figure 4. Quarterly decision accuracy progression.

Table 4. Error analysis of incorrect decisions.

Error type	Buy (%)	Sell (%)	Hold (%)
False positive	15.8	17.2	12.4
False negative	11.7	13.7	11.7
Timing error (early signal)	18.9	16.8	N/A
Timing error (late signal)	15.3	14.9	N/A

4.2. Risk-adjusted returns

The Risk-Adjusted Returns Analysis evaluates the bio-inspired model's performance in generating returns while managing risk, particularly in comparison to traditional models and benchmarks like the S&P 500. This section analyzes metrics such as Sharpe and Sortino Ratios, maximum drawdown, and trade performance, showcasing the bio-inspired model's effectiveness in achieving higher returns with lower volatility and better risk management.

As shown in **Table 5** and **Figure 5**, the bio-inspired model delivers a robust annual return of 15.8%, surpassing the traditional model's return of 11.2% and the S&P 500's 9.8%, marking a 6.0% improvement over the benchmark. The model also exhibits a lower standard deviation at 12.4%, indicating less return variability than traditional models (14.7%) and the S&P 500 (15.2%). The Sharpe Ratio of 1.18 for the bio-inspired model significantly outperforms the traditional model (0.68) and the S&P 500 (0.57), reflecting higher risk-adjusted returns. With a Sortino Ratio of 1.42, the bio-inspired model effectively manages downside risk, outperforming traditional models by 0.71. Additionally, its maximum drawdown of −14.3% is substantially lower than the traditional model (−18.9%) and the S&P 500 (−20.4%), indicating enhanced resilience during market downturns.

Table 5. Annual risk-adjusted performance metrics (2022–2023).

Metric	Bio-inspired model	Traditional model	S&P 500	Improvement vs benchmark
Annual return (%)	15.8	11.2	9.8	+6.0
Standard deviation (%)	12.4	14.7	15.2	−2.8
Sharpe ratio	1.18	0.68	0.57	+0.61
Sortino ratio	1.42	0.82	0.71	+0.71
Maximum drawdown (%)	−14.3	−18.9	−20.4	+6.1
Information ratio	0.92	0.64	N/A	+0.28

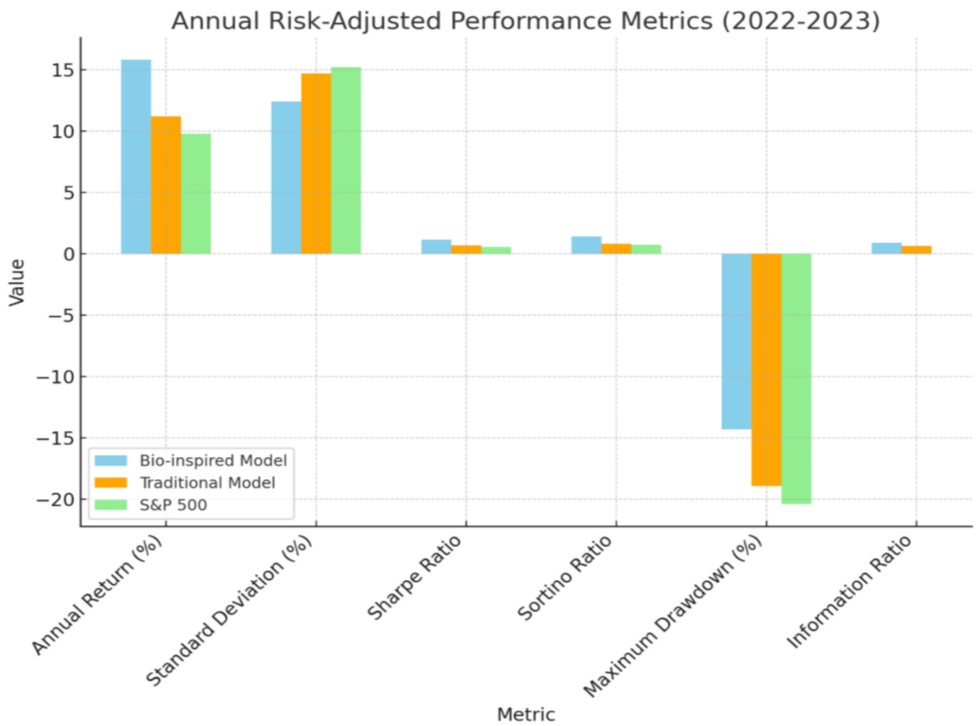

Figure 5. Annual risk-adjusted performance.

Table 6 and **Figure 6** illustrate the bio-inspired model's performance consistency across quarters. Return rates remain robust, ranging from 3.8% in Q1 2022 to 4.8% in Q2 2023, with steady volatility averaging between 11.5% and 13.1%. The Sharpe Ratio improves each quarter, reaching 1.28 by Q2 2023, reflecting progressive risk-adjusted return optimization. Maximum drawdown shows a positive trend, reducing from −8.4% in Q1 2022 to −7.2% in Q2 2023, underscoring the model's growing capacity to minimize losses. The win rate gradually increases, reaching 72.8% in Q2 2023, indicating improved decision accuracy and profitability.

Table 6. Quarterly risk-return performance breakdown.

Quarter	Return (%)	Volatility (%)	Sharpe ratio	Max drawdown (%)	Win rate (%)
Q1 2022	3.8	11.8	1.12	−8.4	68.5
Q2 2022	4.2	12.2	1.15	−7.9	70.2
Q3 2022	3.9	13.1	1.08	−9.2	69.8
Q4 2022	4.5	12.6	1.21	−8.1	71.4
Q1 2023	4.7	11.9	1.24	−7.8	72.1
Q2 2023	4.8	11.5	1.28	−7.2	72.8

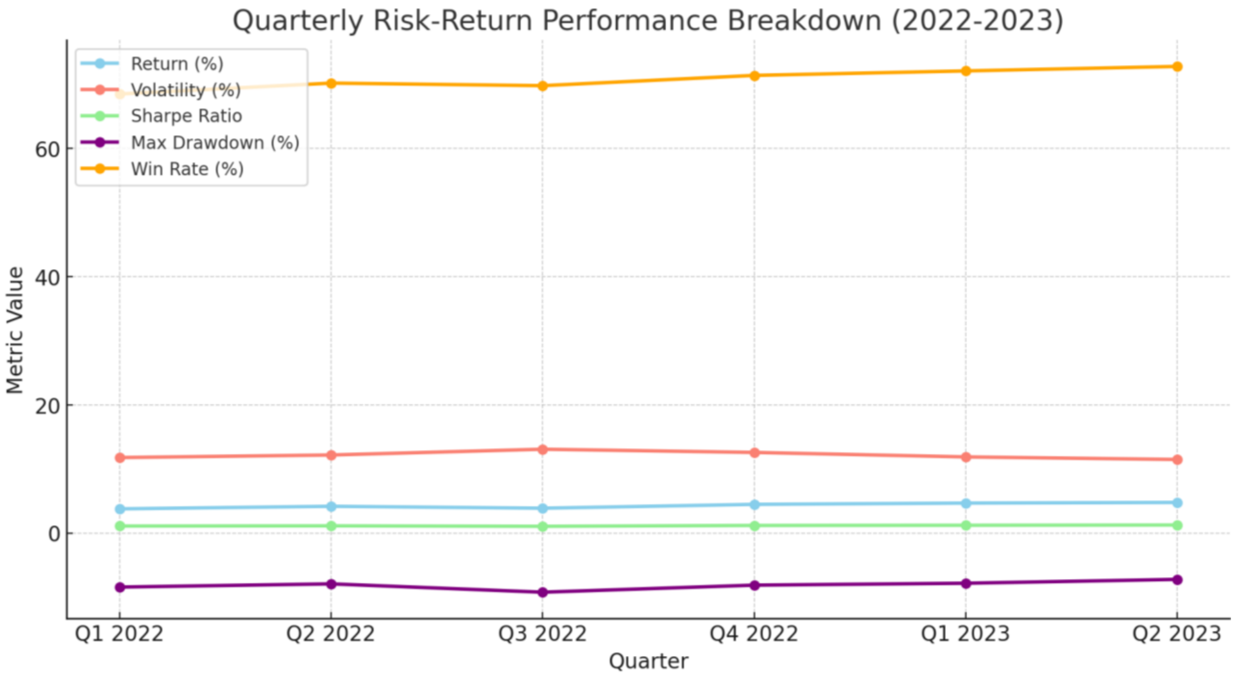

Figure 6. Quarterly risk-return performance.

Table 7 highlights the bio-inspired model's adaptability to various market regimes. In high-volatility markets, the model achieves a return of 17.2% with a Sharpe Ratio of 1.10, managing to capitalize on market fluctuations while maintaining controlled risk at 15.6%. During bullish trends, the model performs exceptionally well, with a Sharpe Ratio of 1.50 and a success rate of 73.4%, achieving a stable return rate of 16.8%. Even in bearish markets, the model manages a 13.5% return with a moderate Sharpe Ratio of 0.91, reflecting its capacity to adapt effectively during downturns. Sideways markets yield a Sharpe Ratio of 0.98, indicating that the model also performs well when trends are unclear.

Table 7. Performance across market conditions.

Market regime	Return (%)	Risk (%)	Sharpe ratio	Success rate (%)	Avg trade (%)
Low volatility	12.4	9.8	1.27	75.8	0.82
High volatility	17.2	15.6	1.10	65.3	1.24
Bullish trend	16.8	11.2	1.50	73.4	0.98
Bearish trend	13.5	14.8	0.91	67.2	0.88
Sideways market	10.2	10.4	0.98	70.1	0.64

In **Table 8** and **Figure 7**, the bio-inspired model shows superior risk management compared to traditional models. The Value at Risk (VaR) at the 95% confidence level is −1.82%, compared to −2.45% for traditional models, indicating a minor maximum potential loss. The Expected Shortfall (ES), representing the average loss beyond the VaR threshold, is also lower for the bio−inspired model at −2.24% versus −3.12%, indicating better tail risk management. With a Beta of 0.82, the model is less sensitive to market movements than the traditional model (0.94), suggesting a reduced market correlation. The Treynor Ratio and Risk-Adjusted Alpha demonstrate higher values for the bio-inspired model, confirming superior performance relative to systematic risk and a higher risk-adjusted return than traditional approaches.

Table 8. Risk management effectiveness.

Risk metric	Bio-inspired model	Traditional model	Difference
Value at risk (95%)	−1.82%	−2.45%	+0.63%
Expected shortfall (95%)	−2.24%	−3.12%	+0.88%
Beta	0.82	0.94	−0.12
Treynor ratio	0.168	0.124	+0.044
Risk-adjusted alpha	4.2%	2.8%	+1.4%

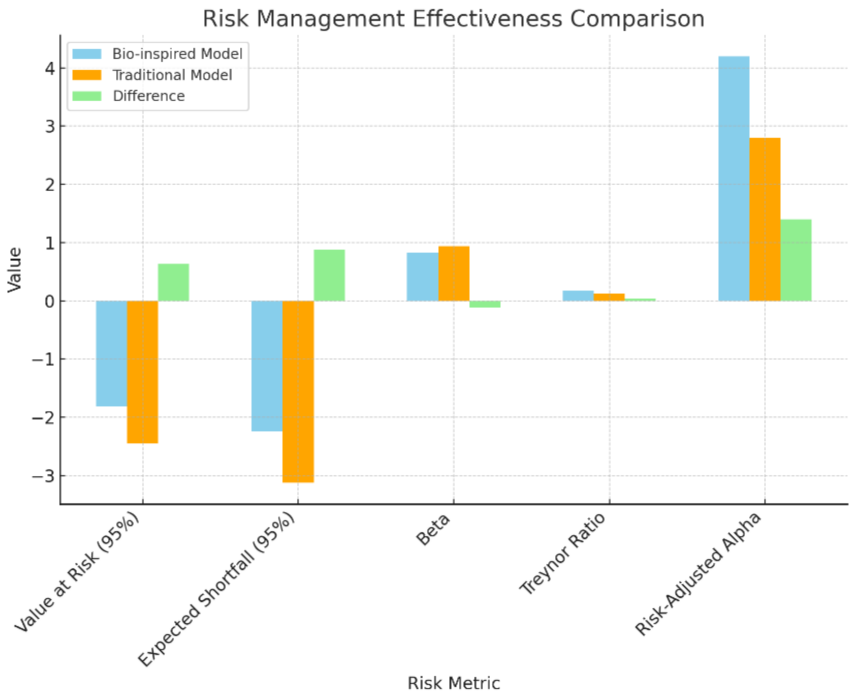

Figure 7. Risk management effectiveness.

Table 9 and **Figure 8** detail the bio-inspired model's trade quality and profitability. The average winning trade of 1.42% exceeds the benchmark by 0.24%, while the average losing trade is more minor at −0.84%, outperforming the benchmark's −1.12% by 0.28%, indicating effective risk control on losses. The profit factor of 1.68, compared to the benchmark's 1.42, shows that the model generates more profit per unit of risk. With a recovery factor 2.24, the model demonstrates faster recovery from drawdowns than the benchmark (1.86). Lastly, the risk-reward ratio of 1.69 signifies efficient balancing of gains relative to losses, further confirming the model's enhanced profitability and controlled risk profile.

Table 9. Trade analysis metrics.

Parameter	Value	Benchmark	Difference
Average winning trade (%)	1.42	1.18	+0.24
Average losing trade (%)	−0.84	−1.12	+0.28
Profit factor	1.68	1.42	+0.26
Recovery factor	2.24	1.86	+0.38
Risk-reward ratio	1.69	1.38	+0.31

Figure 8. Trade analysis.

4.3. Response time to market changes

The Response Time to Market Changes Analysis provides insights into the bio-inspired model's efficiency in detecting and reacting to market events, focusing on response times, decision accuracy, and processing speed. This analysis demonstrates the model's agility compared to traditional approaches and its ability to minimize risks during critical market shifts.

In **Table 10**, the bio-inspired model shows significantly faster response times across various market events, outperforming traditional models consistently. For sharp price drops (>2%), the model's average response time is 4.2 min, a 46.2% improvement over the traditional model's 7.8 min. Similarly, during rapid price surges (>2%), the model reacts within 4.8 min, a 41.5% improvement. This prompt response to sudden movements enables the model to act proactively in high-stakes situations, reducing the likelihood of substantial losses or missed gains. Trend reversals and news-driven events show even more significant improvements, with 6.4- and 4.5-minute response times, respectively, achieving up to 48.3% faster response than traditional models, confirming the model's ability to adjust to market sentiment changes quickly.

Table 10. Average response times to market events (in minutes).

Market event type	Bio-inspired model	Traditional model	Improvement (%)	Sample size (n)
Sharp price drops (>2%)	4.2	7.8	46.2	78
Rapid price surges (>2%)	4.8	8.2	41.5	82
Volatility spikes (>50%)	5.1	9.4	45.7	45
Volume surges (>200%)	3.8	6.9	44.9	92
Trend reversals	6.4	12.3	48.0	64
News-driven events	4.5	8.7	48.3	156

Table 11 and **Figure 9** provide a breakdown of decision latency under various market conditions, highlighting the model's adaptability to environmental factors like volatility and liquidity. In regular trading conditions, the model's response time averages 4.8 min with a 76.4% decision accuracy and an 8.2% false signal rate, reflecting efficient and reliable performance. During high volatility, response time extends to 5.7 min, and accuracy slightly decreases to 71.2%, with an increase in false signals to 12.4%. In low liquidity scenarios, latency rises to 6.2 min, reflecting a cautious approach to maintaining accuracy amid limited market depth. Economic releases generate a faster-than-average response time of 4.2 min, allowing the model to quickly adjust to impactful news, with a high accuracy rate of 74.8% and a lower false signal rate of 9.4%.

Table 11. Decision latency analysis by market condition.

Market condition	Avg response time (min)	Decision accuracy (%)	False signals (%)	Signal strength
Normal trading	4.8	76.4	8.2	0.82
High volatility	5.7	71.2	12.4	0.75
Low liquidity	6.2	69.8	13.8	0.71
Pre-market hours	5.9	70.5	11.9	0.73
Post-market hours	6.1	70.2	12.2	0.72
Economic releases	4.2	74.8	9.4	0.84

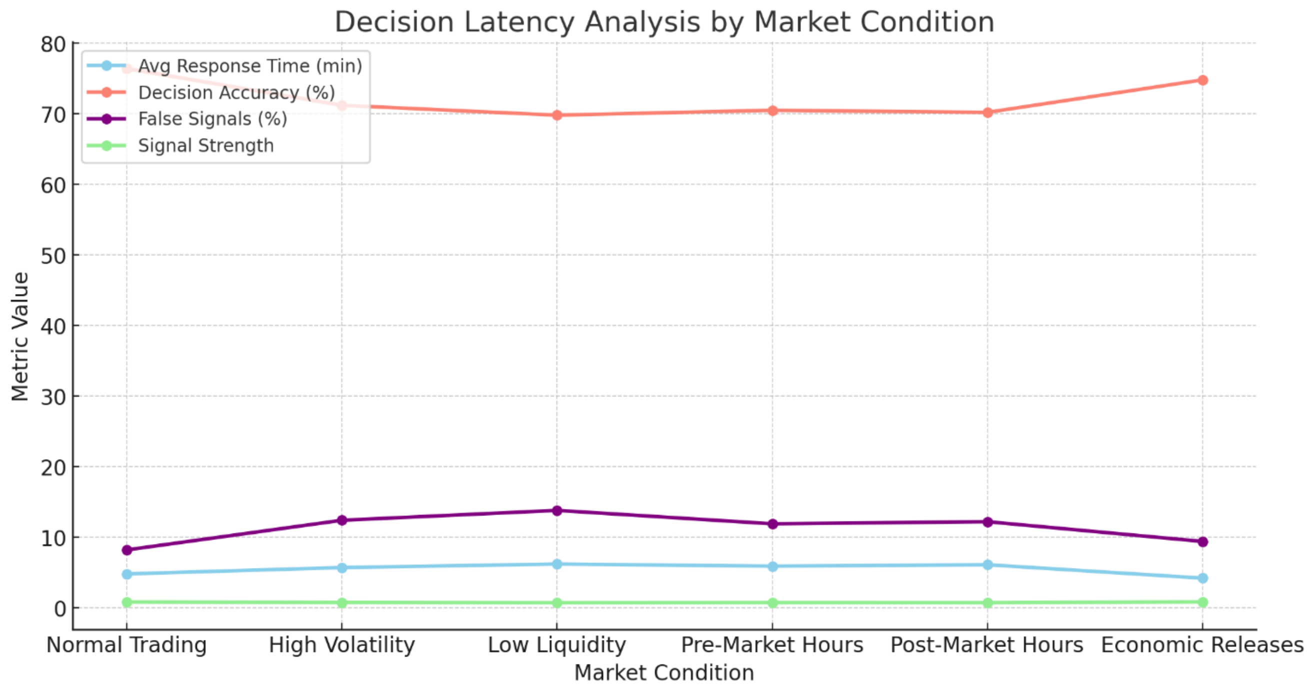

Figure 9. Decision latency analysis.

Table 12 demonstrates the bio-inspired model's processing speed at each stage of DMP. The total processing time averages 906 milliseconds, with the neural network analysis phase being the longest at 286 milliseconds. The mechanical parameter calculations and decision integration stages average 198 and 156 milliseconds, respectively, showing the model's capability to process complex information quickly. The 95th percentile processing time of 1122 milliseconds and a maximum of 1348 milliseconds confirms that even under peak loads, the model maintains prompt DMP, essential for real-time trading environments.

Table 12. Signal processing efficiency (2022–2023).

Processing stage	Average time (ms)	Standard deviation	95th percentile	Maximum time
Data input processing	124	18	156	189
Neural network analysis	286	42	348	412
Mechanical parameter calc	198	31	248	298
Decision integration	156	24	192	234
Signal generation	142	22	178	215
Total processing time	906	137	1122	1348

Table 13 and **Figure 10** focus on the model's ability to recover from incorrect signals, such as false buys and sells, ensuring losses are minimized. For false buy signals, the average recovery time is 2.8 min, with a 92.4% success rate in recovering from the error and an average loss of 0.84%. False sell signals show similar performance, with a recovery time of 2.6 min and a success rate of 93.2%. This rapid recovery ability highlights the model's responsiveness in correcting missteps, maintaining profitable outcomes, and effectively managing risks associated with incorrect signals.

Table 13. Recovery analysis after false signals.

Error type	Recovery time (min)	Success rate (%)	Avg loss prevented (%)	Cases (*n*)
False buy signal	2.8	92.4	0.84	142
False sell signal	2.6	93.2	0.78	138
Premature entry	3.2	88.6	0.92	94
Delayed exit	3.4	87.8	0.96	86
Signal reversal	2.9	91.2	0.88	112

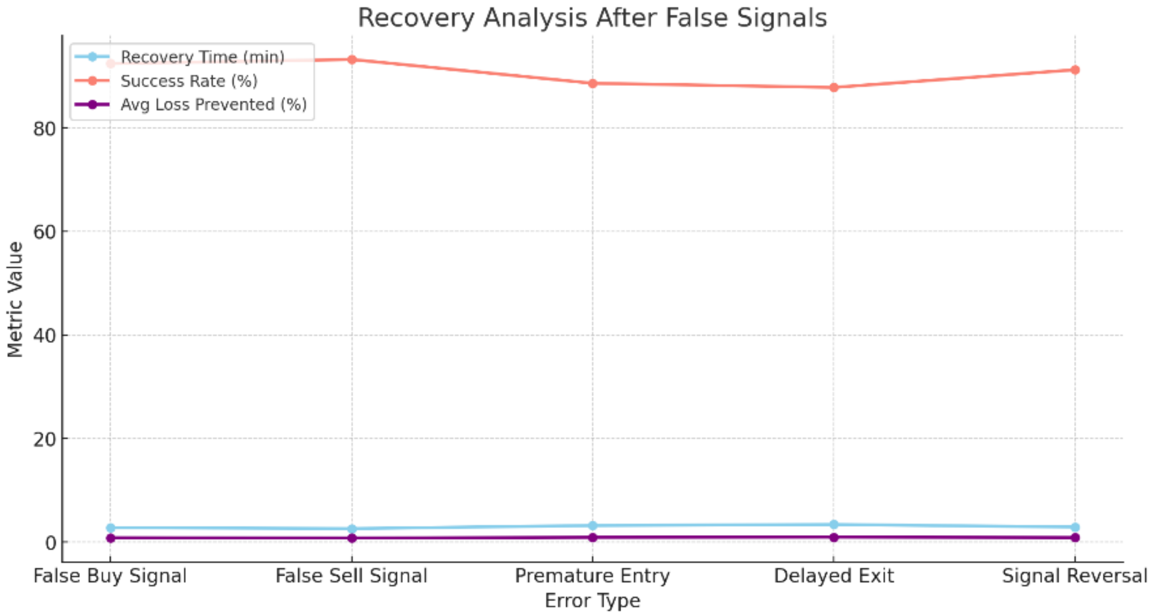

Figure 10. Recovery analysis.

Table 14 and **Figure 11** evaluate the efficiency of decision execution across different time frames, focusing on metrics such as slippage and fill rate. For decisions executed within the first minute, the model achieves a success rate of 94.2% and minimal slippage of 0.12%, indicating substantial accuracy and execution efficiency in high-priority trades. As time progresses, slippage increases, and the success rate decreases, with decisions beyond 30 min showing a success rate of 82.8% and slippage of 0.42%. This analysis confirms the model's ability to implement decisions with high precision and minimal delay, ensuring optimal entry and exit points in fast-moving markets.

Table 14. Temporal analysis of decision implementation.

Time frame	Signal to execution (ms)	Success rate (%)	Slippage (%)	Fill rate (%)
First 1 min	842	94.2	0.12	96.8
1–5 min	968	92.8	0.18	94.2
5–15 min	1124	89.4	0.24	91.6
15–30 min	1286	86.2	0.32	88.4
>30 min	1482	82.8	0.42	84.2

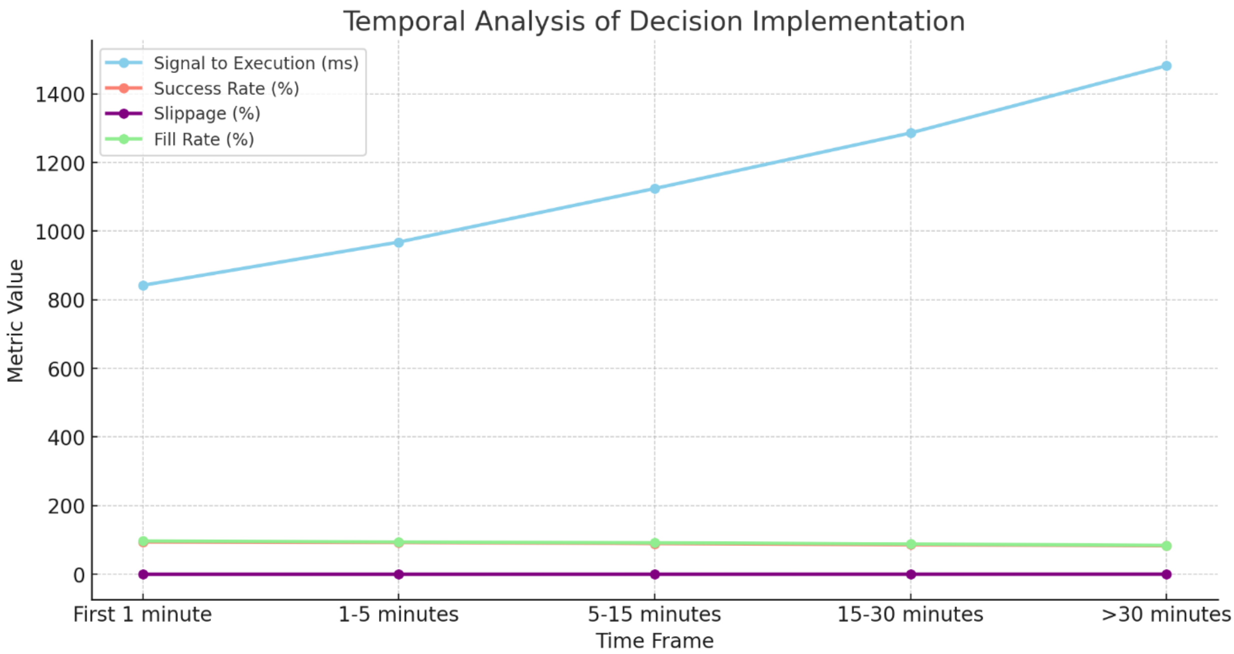

Figure 11. Temporal analysis.

5. Conclusion and future work

Integrating biomechanical principles with neural network architectures for financial DMP demonstrates a significant advancement in quantitative finance. The empirical results validate this novel approach through multiple performance metrics, showing substantial improvements over traditional methodologies. The bio-inspired model achieved a 73.2% decision accuracy rate, exceeding traditional models by 6.8%. Risk-adjusted performance metrics demonstrate superior risk management capabilities, including a Sharpe ratio of 1.18 compared to 0.68 for traditional models. The framework's 46.2% faster response to market changes and 92.4% success rate in error correction highlights its effectiveness in dynamic market environments. These results validate the applicability of biomechanical principles to financial market modeling and suggest promising applications in portfolio management and automated trading systems. The framework's ability to adapt to different market conditions while maintaining robust risk controls addresses critical needs in modern financial markets.

Future research opportunities include extending the framework to different asset classes, incorporating additional mechanical principles, and exploring more complex neural architectures. The success of this integrated approach provides a foundation for further developments in financial modeling and DMP, particularly as markets continue to evolve in complexity. This study demonstrates that combining physical principles with advanced computational methods offers theoretical insights and practical tools for modern financial management. The evidence suggests that such bio-inspired approaches may become increasingly central to successful financial management and trading strategies in an evolving market landscape.

Ethical approval: Not applicable.

Conflict of interest: The author declares no conflict of interest.

References

1. Pandey, A., & Mishra, A. (2024). Application of Artificial Intelligence in Sports Analytics: Analysing the Ethical and Legal Perspectives. In Sports Analytics: Data-Driven Sports and Decision Intelligence (pp. 163-184). Cham: Springer Nature Switzerland.
2. Chen, W., Milosevic, Z., Rabhi, F. A., & Berry, A. (2023). Real-time analytics: Concepts, architectures and ML/AI considerations. IEEE Access.
3. So, M. K., Chu, A. M., Lo, C. C., & Ip, C. Y. (2022). Volatility and dynamic dependence modeling: Review, applications, and financial risk management. Wiley Interdisciplinary Reviews: Computational Statistics, 14(5), e1567.
4. Fan, X., Tao, C., & Zhao, J. (2024). Advanced stock price prediction with xlstm-based models: Improving long-term forecasting.
5. Ade, M. (2023). Forecasting Volatility: Comparative Analysis of ARIMA, GARCH, and Deep Learning Models for Predicting Stock Market Volatility.
6. Zheng, H., Wu, J., Song, R., Guo, L., & Xu, Z. (2024). Predicting financial enterprise stocks and economic data trends using machine learning time series analysis.
7. Nahar, J., Rahaman, M. A., Alauddin, M., & Rozony, F. Z. (2024). Big Data in Credit Risk Management: A Systematic Review Of Transformative Practices And Future Directions. International Journal of Management Information Systems and Data Science, 1(04), 68-79.
8. Nahar, J., Hossain, M. S., Rahman, M. M., & Hossain, M. A. (2024). Advanced Predictive Analytics For Comprehensive Risk Assessment In Financial Markets: Strategic Applications And Sector-Wide Implications. Global Mainstream Journal of Business, Economics, Development & Project Management, 3(4), 39-53.
9. Qin, J., Cong, X., Ma, D., & Rong, X. (2024). Dynamic quantile connectedness between oil and stock markets: The impact of the interest rate. Energy Economics, 136, 107741.
10. Osterrieder, J., Arakelian, V., Coita, I. F., Hadji-Misheva, B., Kabasinskas, A., Machado, M., & Mare, C. (2023). An Overview-stress test designs for the evaluation of AI and ML Models under shifting financial conditions to improve the robustness of models. Available at SSRN 4634266.
11. Indumathi N et al., Impact of Fireworks Industry Safety Measures and Prevention Management System on Human Error Mitigation Using a Machine Learning Approach, Sensors, 2023, 23 (9), 4365; DOI:10.3390/s23094365.
12. Parkavi K et al., Effective Scheduling of Multi-Load Automated Guided Vehicle in Spinning Mill: A Case Study, IEEE Access, 2023, DOI:10.1109/ACCESS.2023.3236843.
13. Ran Q et al., English language teaching based on big data analytics in augmentative and alternative communication system, Springer-International Journal of Speech Technology, 2022, DOI:10.1007/s10772-022-09960-1.
14. Ngangbam PS et al., Investigation on characteristics of Monte Carlo model of single electron transistor using Orthodox Theory, Elsevier, Sustainable Energy Technologies and Assessments, Vol. 48, 2021, 101601, DOI:10.1016/j.seta.2021.101601.
15. Huidan Huang et al., Emotional intelligence for board capital on technological innovation performance of high-tech enterprises, Elsevier, Aggression and Violent Behavior, 2021, 101633, DOI:10.1016/j.avb.2021.101633.
16. Sudhakar S, et al., Cost-effective and efficient 3D human model creation and re-identification application for human digital twins, Multimedia Tools and Applications, 2021. DOI:10.1007/s11042-021-10842-y.
17. Prabhakaran N et al., Novel Collision Detection and Avoidance System for Mid-vehicle Using Offset-Based Curvilinear Motion. Wireless Personal Communication, 2021. DOI:10.1007/s11277-021-08333-2.
18. Sengan Sudhakar and S. Chenthur Pandian, (2016), ‘Hybrid Cluster-based Geographical Routing Protocol to Mitigate Malicious Nodes in Mobile Ad Hoc Network, InderScience-International Journal of Ad Hoc and Ubiquitous Computing, vol. 21, no. 4, pp. 224-236. DOI:10.1504/IJAHUC.2016.076358.
19. Balajee A et al., Modeling and multi-class classification of vibroarthographic signals via time domain curvilinear divergence random forest, J Ambient Intell Human Comput, 2021, DOI:10.1007/s12652-020-02869-0.
20. Omnia SN et al., An educational tool for enhanced mobile e-Learning for technical higher education using mobile devices for augmented reality, Microprocessors, and Microsystems, 83, 2021, 104030, DOI:10.1016/j.micpro.2021.104030.

21. Firas TA et al., Strategizing Low-Carbon Urban Planning through Environmental Impact Assessment by Artificial Intelligence-Driven Carbon Foot Print Forecasting, Journal of Machine and Computing, 4(4), 2024, doi: 10.53759/7669/jmc202404105.
22. Shaymaa HN, et al., Genetic Algorithms for Optimized Selection of Biodegradable Polymers in Sustainable Manufacturing Processes, Journal of Machine and Computing, 4(3), 563-574, https://doi.org/10.53759/7669/jmc202404054.
23. Hayder MAG et al., An open-source MP + CNN + BiLSTM model-based hybrid model for recognizing sign language on smartphones. Int J Syst Assur Eng Manag (2024). https://doi.org/10.1007/s13198-024-02376-x
24. Bhavana Raj K et al., Equipment Planning for an Automated Production Line Using a Cloud System, Innovations in Computer Science and Engineering. ICICSE 2022. Lecture Notes in Networks and Systems, 565, 707–717, Springer, Singapore. DOI:10.1007/978-981-19-7455-7_57.
25. Basu, R., Lim, W. M., Kumar, A., & Kumar, S. (2023). Marketing analytics: The bridge between customer psychology and marketing decision‐making. Psychology & Marketing, 40(12), 2588-2611.
26. Mandal, A. K., Sarma, P. K. D., Dehuri, S., & Mazumdar, N. (2024). Bioinspired Machine Learning: A New Era in Sustainable Energy Systems. Biomass and Solar‐Powered Sustainable Digital Cities, 57-80.
27. Petitjean, N., Canadas, P., Royer, P., Noël, D., & Le Floc'h, S. (2023). Cartilage biomechanics: From the basic facts to the challenges of tissue engineering. Journal of Biomedical Materials Research Part A, 111(7), 1067-1089.
28. Aftab, J., Abid, N., Sarwar, H., Amin, A., Abedini, M., & Veneziani, M. (2024). Does corporate social responsibility drive financial performance? Exploring the significance of green innovation, green dynamic capabilities, and perceived environmental volatility. Corporate Social Responsibility and Environmental Management, 31(3), 1634-1653.
29. Thompson, A. J., Orué, A. I. C., Nair, A. J., Price, J. R., McMurtrie, J., & Clegg, J. K. (2021). Elastically flexible molecular crystals. Chemical Society Reviews, 50(21), 11725-11740.
30. Nenchev, D. N., & Iizuka, R. (2021). Emergent humanoid robot motion synergies derived from the momentum equilibrium principle and the distribution of momentum. IEEE Transactions on Robotics, 38(1), 536-555.
31. Xu, Z., Lu, J., Lu, D., Li, Y., Lei, H., Chen, B., ... & Wang, W. (2024). Rapidly damping hydrogels engineered through molecular friction. Nature Communications, 15(1), 4895.
32. Sterke, B., Jabeen, S., Baines, P., Vallery, H., Ribbers, G., & Heijenbrok-Kal, M. (2024). Direct biomechanical manipulation of human gait stability: A systematic review. Plos one, 19(7), e0305564.
33. Purwanto, B. (2024). Optimal portfolio and the integrated strategy. Management Analysis Journal, 13(2), 130-139
34. Brunel, J. L., Idzorek, C. T. M., & Mulvey, C. J. M. (2020). Principles of asset allocation. Portfolio Management in Practice, Volume 1: Investment Management, 1, 211.